PeptideScience
THE AMERICAN PEPTIDE SOCIETY JOURNAL

# Special Issue: Peptide Engineering Meeting 8

Guest Editors: Prof. Beate Koksch (Freie Universität Berlin), Dr Joel P. Schneider (National Institutes of Health), Prof. Peter H. Seeberger (Max Planck Institute of Colloids and Interfaces) and Prof. Claudio Toniolo (University of Padova)


## EDITORIALS



## REVIEWS



## FULL PAPERS

PeptideScience
THE AMERICAN PEPTIDE SOCIETY JOURNAL

# Special Issue: Peptide Engineering Meeting 8

Guest Editors: Prof. Beate Koksch (Freie Universität Berlin), Dr Joel P. Schneider (National Institutes of Health), Prof. Peter H. Seeberger (Max Planck Institute of Colloids and Interfaces) and Prof. Claudio Toniolo (University of Padova)


Conversion of cationic amphiphilic lytic peptides to cell-penetration peptides
Hao-Hsin Yu, Kentarou Sakamoto, Misao Akishiba, Naoki Tamemoto, Hisaaki Hirose, Ikuhiko Nakase, Miki Imanishi, Fatemeh Madani, Astrid Gräslund and Shiroh Futaki, *Peptide Science* 2020, doi: 10.1002/pep2.24144

Spiegelmeric 4*RIS*-hydroxy/amino-L/D-prolyl collagen peptides: Conformation and morphology of self-assembled structures
Shahaji H. More and Krishna N. Ganesh, *Peptide Science* 2020, doi: 10.1002/pep2.24140

Received: 1 April 2019 | Revised: 10 June 2019 | Accepted: 21 June 2019

DOI: 10.1002/pep2.24127

FULL PAPER

PeptideScience WILEY

# Halogen bonding as a key interaction in the self-assembly of iodinated diphenylalanine peptides

Andrea Pizzi[1] | Luca Catalano[1] | Nicola Demitri[2] | Valentina Dichiarante[1] | Giancarlo Terraneo[1] | Pierangelo Metrangolo[1]

[1]Department of Chemistry, Materials, and Chemical Engineering "Giulio Natta", Politecnico di Milano, Via Luigi Mancinelli 7, 20131 Milano, Italy

[2]Elettra-Sincrotrone Trieste, S.S. 14 Km 163.5 in Area Science Park, 34149 Basovizza, Trieste, Italy

**Correspondence**
Pierangelo Metrangolo, Laboratory of Supramolecular and Bio-Nanomaterials (SupraBioNanoLab), Department of Chemistry, Materials, and Chemical Engineering "Giulio Natta," Politecnico di Milano, Via Luigi Mancinelli 7, Milano 20131, Italy.
Email: pierangelo.metrangolo@polimi.it

**Funding information**
European Research Council, Grant/Award Numbers: Grant Agreement Number 307108, Grant Agreement Number 789815

## Abstract

The diphenylalanine peptide FF ($H_2N$-Phe-Phe-COOH) is a simple building-block that has been extensively studied for multiple purposes. Among the many possible mutations finalized to tailor specific functions and properties of FF-based materials, halogenation was marginally considered despite the huge changes it confers to molecular self-assembly. Here, we report a detailed study on the role of halogenation, specifically iodination, in the aggregation behavior of iodine-modified FF dipeptides. Single-crystal X-ray structures of mono-iodinated—F(I)F—and bis-iodinated—F(I)F(I)—diphenylalanine reveal that halogen atoms exert a key role in the packing features of these compounds. Specifically, halogen bonding provides additional stability to the dry interfaces formed by the aromatic rings, providing a contribution in the solid-state packing of these dipeptides. The structural evidence of halogen bonding as crucial noncovalent interaction confirms the great potential of halogenation as supramolecular tool for peptide-based systems.

**KEYWORDS**
diphenylalanine peptide, halogenated peptides, halogenation, halogen bond, iodination, single-crystal X-ray structure, structural studies

## 1 | INTRODUCTION

Molecular self-assembly earned a prominent position among the possible strategies to produce nanostructures with various morphologies.[1] The simplicity of this approach, based on the spontaneous occurrence of noncovalent interactions leading to supramolecular objects (i.e., hydrogen bonding, electrostatic forces, and aromatic interactions), resulted in a wide range of spreading of molecular self-assemblies in several application fields.[2,3] The rational design of the starting molecular structures producing self-assembled architectures takes often inspiration from Nature, which offers the best synthesis of building blocks' simplicity, with complexity of the resulting structure and its related functionality. Among the many examples offered by Nature, the countless combinations of the 20 amino acids give rise to proteins that fold into secondary, tertiary, and quaternary structures to exert specific functions.[4] Because of their huge chemical variety, amino acids represent a robust starting point for the design of new biomimetic supramolecular structures.[5] Combining amino acids into small peptides, polypeptides, or proteins opened up a revolution in the context of nanotechnologies. Notably, in the case of peptides, features like essential structural design, ease of synthesis, and easy access to chemical modification add to excellent biocompatibility, as well as strong chemical stability.[6–8] These advantages made peptides a favorite tool even for applications, which are not strictly related to biology, that is, nanoelectronics[9] and energy storage.[10] Peptides offer a wide range of possible supramolecular morphologies (fibers, rods, tubes, spheres, and plates),[11] which are firmly sequence-specific or tunable through the application of external stimuli such as temperature, pH variation, or electric field.[6] Amyloid fibrils have been for long the most extensively studied self-assembled

  

objects because of their correlation with important neurodegenerative disorders[12] and outstanding mechanical properties,[13] the latter being attractive for high-performance nanomaterials.[14] Many peptide sequences were investigated aiming to reproduce in small molecular motifs the remarkable self-association typical of amyloid proteins. In this regard, both experimental[15,16] and computational studies[17] clarified the importance of aromatic interactions in the aggregation process of amyloid materials, identifying the dipeptide diphenylalanine (FF) as a core motif, whose presence in longer sequences triggers the fibrillation process. Reches and Gazit reported the ability of diphenylalanine peptide to form well-ordered nanotubes from aqueous solutions, and their application as molds for metal nanowires.[18] From there, the scientific interest related to this peptide grew exponentially; indeed, recent research works showed the use of diphenylalanine for antibacterial agents,[19] piezoelectric components for energy harvesters,[20–22] optical waveguides,[23] hydrogels,[24] drug delivery systems,[25] and integration of metal nanocomposites.[26] Taking this aromatic dipeptide as elementary motif, many chemical modifications were investigated to control the morphology of the self-assembled nano-objects, tailoring the system for the desired application.[27] Among the possible structural changes, iodination at the *para*-position of both aromatic rings led to the formation of tubular structures having a similar morphology to the ones formed by the unmodified dipeptide.[28] Although halogenation is just a single point mutation, it confers many different physical and chemical properties that go far beyond a lower solubility. Indeed, it enlarges the set of possible noncovalent interactions that drive the molecular self-assembly process. Among these interactions, one of the most studied due to its strength, specificity, and directionality is halogen bonding (XB)[29]; due to the anisotropic distribution of the electron density in highly polarizable halogen atoms, they can behave as electrophilic species, amplifying the potential interaction pattern of the motif containing this modification.

In the context of noncovalent interactions involving halogen atoms, halogen-halogen contacts can occur according to two different geometries: type I and type II. Considering a generic halogen-halogen contact $R - X_1 \cdots X_2 - R$ (where X is a halogen atom) and the angles $\theta_1$ ($R - X_1 \cdots X_2$) and $\theta_2$ ($R - X_2 \cdots X_1$), type I is defined as a symmetrical interaction where $\theta_1 = \theta_2$, while type II is a bent interaction where $\theta_1 \approx 180^\circ$ and $\theta_2 \approx 90^\circ$. The latter is a proper halogen bond since the interaction occurs between the electrophilic area of a halogen atom and the electron-rich belt of another halogen atom. Type I is instead a geometry-based contact that is not considered a halogen bond according to the IUPAC definition.[29] Iodination of proteins and peptides is a common strategy to help phase determination and structure solution in X-ray diffraction experiments, thanks to the anomalous scattering of iodine. In the case of high molecular weight proteins, the effect of iodine on the resulting structure is negligible since the self-assembly is driven by a multiplicity of other noncovalent interactions. However, in the case of small peptides, iodination makes the difference affecting their overall aggregation behavior; in this latter case, halogenation may be also exploited to tune the supramolecular properties of a system.

Recent works from our group reported the impact of halogenation in the self-assembly properties of simple organic systems containing phenylalanine residues. Studies based both on a single phenylalanine[30] and short peptide sequences[31–35] confirmed that halogenation enhances the self-aggregating propensity compared to the corresponding nonhalogenated systems, this proclivity being a function of halogen polarizability. Moreover, in the case of amyloid peptide fragments, several kinds of nanostructures were observed by changing number, position, and nature of the halogen substitution.[33] Notably, the role of the halogen atom in the self-assembly process of these systems was determined at the atomic level through single-crystal X-ray diffraction, revealing the occurrence of halogen bonding as key noncovalent interaction. In particular, one of the peptides we investigated—KLVFF, the core sequence of the polypeptide Aβ40—confirmed the great potential of halogenation on the FF motif in tuning of the peptide self-assembly properties. For this reason, and also considering the lack of a structural insight about the role of halogenation in the supramolecular behavior of iodinated FF dipeptides, here we report the high-resolution single-crystal X-ray structure of different iodinated diphenylalanine peptides. A detailed structural study of the packing features of both mono-iodinated and bis-iodinated derivatives of FF revealed the role of halogen atoms and halogen bonding in different solvents. Considering the low complexity of this dipeptide, combined with the frequent occurrence of XBs in several crystallization conditions, we infer that halogen bonding cannot be overlooked as key interaction for the supramolecular nanostructures formed by these iodinated systems.

## 2 | MATERIALS AND METHODS

Peptides were purchased from Biopeptek Pharmaceuticals LLC, USA. Ion-spray mass spectrometry confirmed the integrity of all peptides, while purity (≥ 98%) was determined by reverse-phase high-pressure liquid chromatography.

### 2.1 | Infrared spectroscopy

Infrared spectra were obtained at room temperature using the attenuated total reflectance module of a Nicolet iS50 Fourier-transform infrared (FT-IR) spectrometer, equipped with a deuterated triglycine sulfate detector. Peptides were analyzed under different conditions:

1. in bulk without any previous treatment
2. solid films resulting from evaporation of peptide solutions prepared in different solvents (dimethyl sulfoxide [DMSO], water/DMSO 98:2)

Spectra represent an average of 64 scans recorded in a single beam mode with a 1 $cm^{-1}$ resolution and corrected for the background.

## 2.2 | Peptides crystallization

$H_2N$-(*p*-IodoPhe)-(*p*-IodoPhe)-COOH, that is, F(I)F(I), was obtained as solvated species by dissolving the peptide (100 mg/mL) in DMSO and pyridine. The crystals suitable for single-crystal X-ray diffraction were obtained after 5 months of slow evaporation.

$H_2N$-(*p*-IodoPhe)-Phe-COOH, that is, F(I)F, was obtained as solvated species by dissolving the peptide in water (1 mg/mL) and pyridine (5 mg/mL). The crystals suitable for single-crystal X-ray diffraction were obtained after 2 months of slow evaporation. For all samples, the crystals used for data collection were extremely thin and generally twinned, thus affecting the maximum resolution of the analysis.

## 2.3 | Scanning electron microscopy

Scanning electron microscopy (SEM) analysis was performed using a Cambridge Stereoscan 360 operating at 20 kV. Freshly prepared peptide solutions (100 mg/mL in DMSO and 2 mg/mL in water/DMSO 98:2) were dried directly on steel stubs and then sputter-coated with silver-palladium before analysis.

## 2.4 | Transmission electron microscopy

Transmission electron microscopy (TEM) images were acquired by using a DeLong America LVEM5, equipped with a field emission gun and operating at 5 kV. Samples were prepared by placing 5 μL of freshly prepared peptide solution (2 mg/mL in water/DMSO 98:2) on 200 mesh carbon-coated copper grids, leaving the drop on the grid surface for 1 min and finally removing the excess of solvent.

## 2.5 | X-ray crystallography data acquisition

Data collection of F(I)F_Water solvate was performed at the X-ray diffraction beamline (XRD1) of the Elettra Synchrotron, Trieste (Italy).[36] The crystals were dipped in perfluoropolyether Fomblin oil (Sigma Aldrich, Saint Louis, USA) and mounted on the goniometer head with kapton loops (MiTeGen, Ithaca, USA). Complete data sets were collected at 100 K (nitrogen stream supplied through an Oxford Cryostream 700—Oxford Cryosystems Ltd., Oxford, UK) using a rotating crystal method. Data were acquired using a monochromatic wavelength of 0.700 Å on a Pilatus 2 M hybrid-pixel area detector (DECTRIS Ltd., Baden-Daettwil, Switzerland). The diffraction data were indexed and integrated using XDS.[37] Crystals appear as thin colorless needles prone to radiation damage, as previously reported for other halogenated molecules.[38,39] The structures were solved by the dual space algorithm implemented in the SHELXT code.[40] Fourier analysis and refinement were performed by the full-matrix least-squares method based on $F^2$ implemented in SHELXL (Version 2018/3).[41] The Coot program was used for modeling.[42]

X-ray data collections of F(I)F(I) crystal structures were performed using a Bruker APEX-II diffractometer (equipped with a sealed tube and a CCD detector) with Mo-Kα radiation ($\lambda$ = 0.71073 Å). The crystal structure of F(I)F_Pyridine solvate was collected on a Bruker APEX-II diffractometer equipped with a sealed tube and a CCD detector using Cu-Kα radiation ($\lambda$ = 1.5418 Å). The crystals were cryocooled (103 K) during data collection using a Bruker KRYOFLEX device. The crystal structures were solved by a direct method and refined against $F^2$ using SHELXL97 and OLEX2.[43,44] Packing diagrams were generated using Mercury.[45] The nonhydrogen atoms were refined anisotropically, and hydrogen atoms were positioned geometrically.

The main crystallographic data for F(I)F and F(I)F(I) are reported in Table 1 and detailed in the following paragraphs.

# 3 | RESULTS AND DISCUSSION

Since we have previously demonstrated that in a peptide endowed with a diphenylalanine moiety (KLVFF) halogenation affects the self-assembly by changing both position and number of the halogen atoms, we studied two different iodinated FF dipeptides. The first is a peptide having an iodine atom at the *para*-position of both phenylalanine residues—F(I)F(I)—which was previously studied by Reches and Gazit.[28] The second is a peptide having a single iodine atom on the aromatic residue at the N-terminus—F(I)F—(Figure 1). Mono-iodination on the C-terminus—FF(I)—was not studied, since halogenation in this position was proved to do not have an active role in the self-assembly, as demonstrated by the crystal structure of KLVFF(I).[34]

Aiming to have a preliminary confirmation on the structural features and the possible contribution of halogen bonding in the solid-state assembly of the iodinated dipeptides F(I)F and F(I)F(I), FT-IR spectra under different experimental conditions were studied: (a) bulk powders; (b) solid films resulting from the evaporation of a DMSO solution; and (c) solid films resulting from the evaporation of a water/DMSO 98:2 solution. A changing in the FT-IR signature is expected moving from the commercial bulk powders to the evaporated peptide solutions, where the compounds are expected to self-assemble through solvent mediation. Some of us reported that a red-shift combined with an intensity enhancement of the C-I stretching band in the far-IR region is a distinct signature of the presence of halogen bond.[46] Although in this region the interpretation of spectra is difficult because of complexity and low intensity of the IR bands, a small red-shift of the C-I stretching band was observed for both F(I)F(I) and F(I)F. In particular, the bulk powder of the bis-iodinated peptide showed hints of signals at 212 and 208 $cm^{-1}$, while distinct peaks at 210 $cm^{-1}$ and 204 $cm^{-1}$ are present in the spectrum of the evaporated DMSO solution (Figure 2). The same signals are further red-shifted at 209 and 203 $cm^{-1}$ in the case of the evaporated water/DMSO solution, indicating that in this solvent the contribution of halogen bonding should be more pronounced than in pure DMSO. A similar trend can be observed also for the mono-iodinated compound (Figure S1).

The red-shifts here noticed are not remarkable as in previously reported co-crystals consisting of iodoperfluoro aromatics and strong halogen-bond acceptors. However, these results suggest the

**TABLE 1** Crystallographic data for the structures of F(I)F and F(I)F(I) presented in this work

| Name | F(I)F_Water | F(I)F_Py | F(I)F(I)_Py | F(I)F(I)_DMSO |
|---|---|---|---|---|
| CCDC number | 1898390 | 1899893 | 1899944 | 1899938 |
| Formula | $(C_{18}H_{17}IN_2O_2)2(H_2O)$ | $C_{18}H_{19}IN_2O_3(C_5H_5N)$ | $(C_{18}H_{18}I_2N_2O_3)(C_5H_5N)(H_2O)$ | $(C_{18}H_{18}I_2N_2O_3)(C_2H_6OS)$ |
| F.W. | 456.27 | 517.35 | 661.26 | 642.30 |
| Cryst. system | Monoclinic | Orthorhombic | Orthorhombic | Orthorhombic |
| Space group | $P\,2_1$ | $P2_12_12_1$ | $P2_12_12_1$ | $P2_12_12_1$ |
| $Z$ | 4 | 4 | 4 | 4 |
| $a$ (Å) | 19.626 (4) | 5.0116 (5) | 5.7436 (14) | 5.3056 (4) |
| $b$ (Å) | 4.730 (1) | 16.407 (2) | 12.805 (3) | 16.0912 (11) |
| $c$ (Å) | 20.447 (4) | 27.413 (3) | 33.539 (7) | 27.134 (2) |
| $\alpha$ (°) | 90 | 90 | 90 | 90 |
| $\beta$ (°) | 95.53 (3) | 90 | 90 | 90 |
| $\gamma$ (°) | 90 | 90 | 90 | 90 |
| $V$ (Å$^3$) | 1889.3 (7) | 2254.0 (4) | 2466.7 (10) | 2316.5 (3) |
| $T$ (K) | 100 | 100 | 103 | 103 |
| $D_{calc}$ (g/cm$^3$) | 1.604 | 1.525 | 1.781 | 1.8415 |
| $\mu$ (mm$^{-1}$) | 1.657 | 11.40 | 2.583 | 2.833 |
| Measured reflns | 15 274 | 6708 | 34 196 | 14 190 |
| Indep. reflns | 8052 | 2806 | 3436 | 3161 |
| $R_1[I > 2\text{sigma}(I)]$ | 0.0743 | 0.097 | 0.0453 | 0.0440 |
| $wR_2$ (all data) | 0.2167 | 0.269 | 0.0713 | 0.0760 |
| $\Delta\rho_{max,\ min}$ (eÅ$^{-3}$) | 1.879, −1.802 | 1.12, −2.50 | 0.951, −0.778 | 1.1947, −1.1217 |
| Goodness of Fit | 0.929 | 1.06 | 1.109 | 0.9443 |

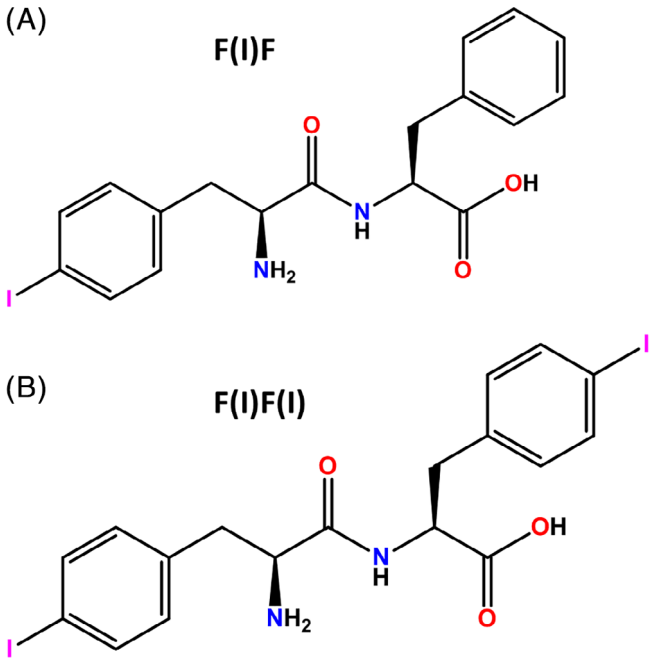


**FIGURE 1** Chemical structures of the iodinated derivatives of the FF sequence studied in this work. A, F(I)F. B, F(I)F(I)

involvement of XBs also in the case of weakly activated iodine atoms introduced in more complex systems, where the competition of other noncovalent interactions like hydrogen bond is not negligible. As a further confirmation of the strong, simultaneous contribution of hydrogen bond in the solid-state packing, we focused also on the changes of amide I region (1600-1700 cm$^{-1}$), associated with the stretching vibration of the carbonyl group. As expected, both dipeptides show a consistent red-shift of the IR signal, moving from bulk powders to the evaporated solutions of DMSO and water/DMSO (Figure S2-3), the latter having the amide I peak at lower frequencies; this variation indicates that the electron density associated with the carbonyl oxygen is depleted by the interaction with an electropositive moiety,[47,48] likely a hydrogen atom.

The morphology of the self-assembled objects formed in the solid state by the same samples analyzed through FT-IR spectroscopy was assessed with SEM and TEM analysis (Figure 3).

As expected, varying the number of iodine atoms deeply changed the resulting nanostructure. Indeed, in pure DMSO, the bis-iodinated peptide forms tubular structures (Figure 3A), while the mono-iodinated one assembles in thick ribbons and lamellar architectures (Figure 3D). Different morphologies were obtained from water/DMSO samples as well, confirming that the diverse aggregation behavior is mainly due to halogen substitution and not strictly related to the solvent. Nanotubes similar to those obtained in pure DMSO were obtained also in water/DMSO for F(I)F(I) (Figure 3B,C), as previously reported for the same compound.[28] Notably, in water/DMSO, entangled networks of thin fibrils were noticed in addition to lamellar structures for F(I)F (Figure 3E,F), proving that monohalogenation on

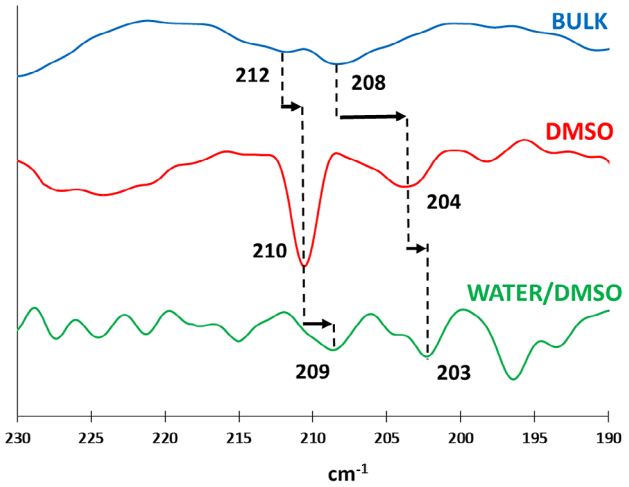


**FIGURE 2** Enlarged region (190-230 $cm^{-1}$) of the far-IR spectra of F(I)F(I) compound under different experimental conditions: (a) bulk powders (blue line); (b) solid film obtained after evaporation of a DMSO solution (red line); (c) solid film obtained after evaporation of a water/DMSO solution (green line)

the *N*-terminal phenylalanine residue confers the highest fibrillation propensity. On the basis of the FT-IR results, hinting the involvement of halogen atoms in the solid-state assembly, and after imaging different nanoarchitectures upon changing the halogenation scheme, further structural characterization at the atomic level was needed to definitely prove the contribution of halogen bonding in the interaction pattern driving the dipeptide aggregation. Crystallization trials of both F(I)F(I) and F(I)F were performed in pure organic solvents due to the low solubility in water of these compounds, especially the bis-iodinated one. For all samples, the crystals used for data collection were extremely thin and generally twinned, thus affecting the maximum resolution of the analysis. We were not successful in obtaining higher quality crystals even after extensive crystallization trials due to intrinsic propensity of the molecular species to form small and poorly diffracting crystals. Only for the mono-iodinated compound we were able to grow crystals in pure water, although in this case synchrotron radiation was necessary to have good diffraction data.

F(I)F was successfully crystallized from water and from pyridine. In water, the dipeptide crystallizes in the chiral monoclinic $P2_1$ space group with two molecules in the asymmetric unit, while in pyridine it crystallizes in the orthorhombic $P2_12_12_1$ space group, with a single peptide molecule in the asymmetric unit (Figure 4).

In both crystal structures, the dipeptide monomers adopt an extended parallel β sheet conformation, stabilized by N-H···O hydrogen bonds involving the amide groups of nearby strands. The β sheets are much more compact in the crystal structure in water, with an average N···O distance of 2.87 Å; in pyridine, the N···O distance is 3.44 Å. These hydrogen-bonded stacks are perfectly in-register, diversely to the molecular stacking observed in two FF structures reported in the CSD (IFABEW and OREVAK).[49–51] Electrostatic interactions links C-terminals carboxylate and protonated N-terminals of flanked molecules (shorter $O^{-}\cdots N^{+}$ distance is 2.71 Å in water, 2.78 Å in pyridine), allowing lateral stabilization between adjacent β sheets (Figure 5). The aromatic residues lie on the same side with respect to the backbone in the water solvate, similarly to IFABEW and OREVAK, which were obtained from the same solvent. Differently, the phenyl rings are located on the opposite sides in the pyridine solvate due to the presence of solvent molecules hydrogen bonded to the N-terminal (N1···N3 distance 2.80 Å).

The orientation of the aromatic moieties in the F(I)F water solvate promotes the formation of extended hydrophobic interfaces, involving the

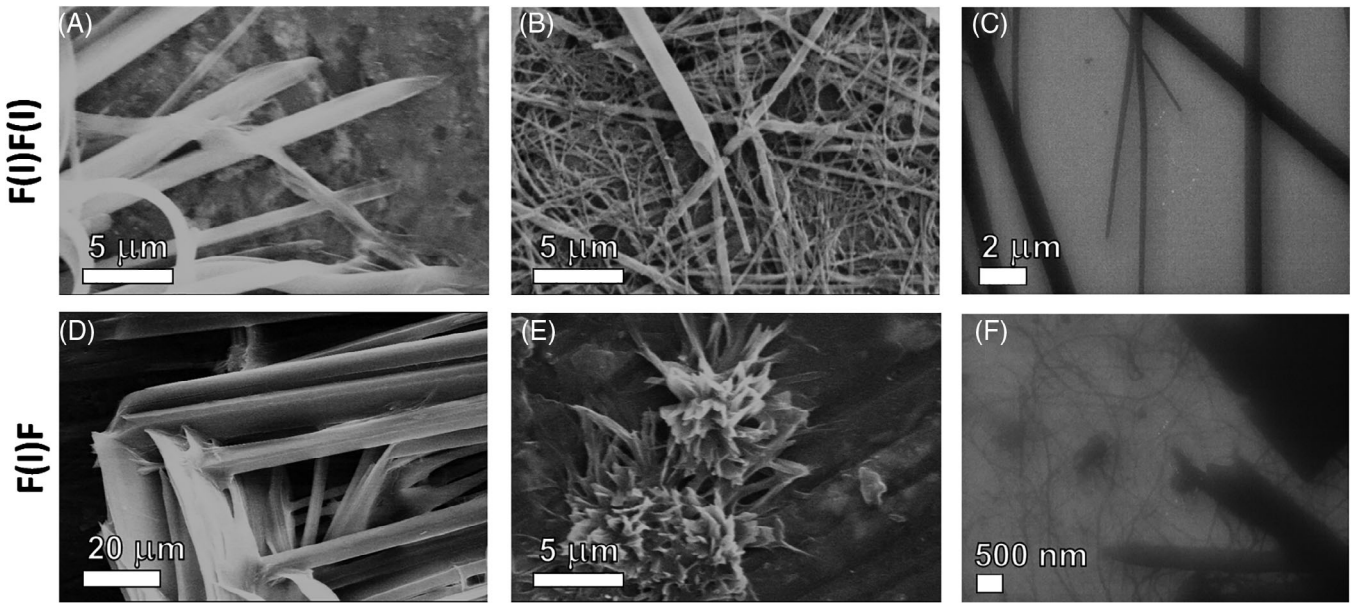


**FIGURE 3** Electron microscopy images of iodinated FF derivatives: A, SEM of F(I)F(I) from DMSO; B, SEM of F(I)F(I) from water/DMSO; C, TEM of F(I)F(I) from water/DMSO; D, SEM of F(I)F from DMSO; E, SEM of F(I)F from water/DMSO; F, TEM of F(I)F from water/DMSO

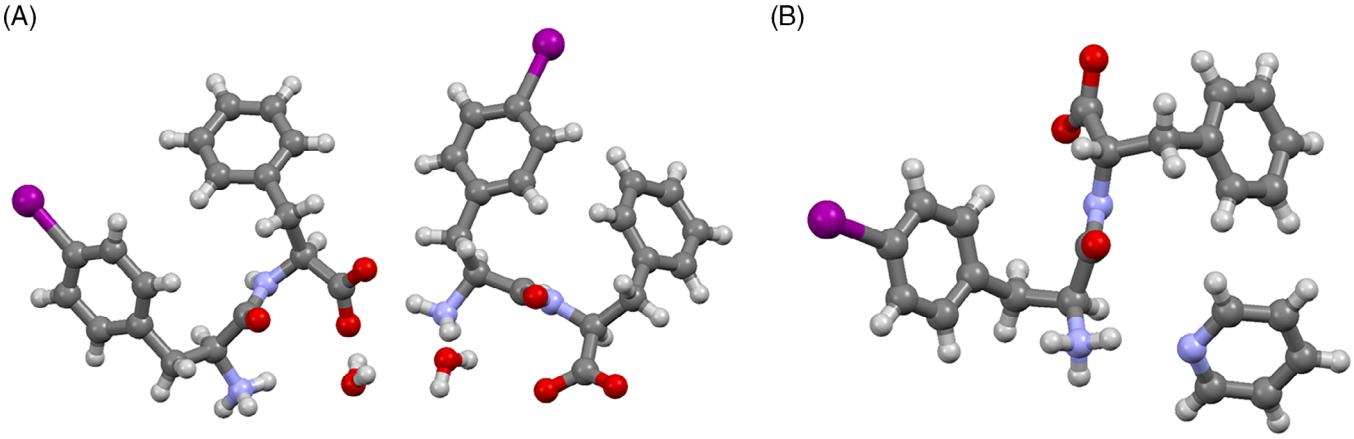


**FIGURE 4** Asymmetric unit content for of F(I)F crystal structures. A, water solvate of F(I)F; B, pyridine solvate of F(I)F. Color code: C, gray; O, red; N, violet; I, purple; H, white

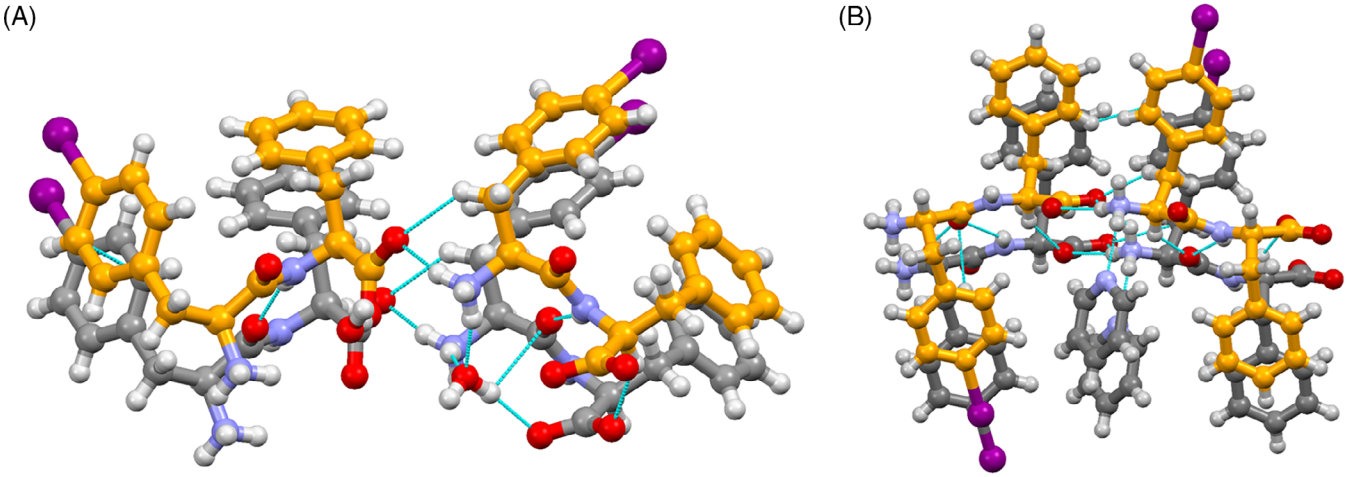


**FIGURE 5** Crystal structures of F(I)F. Stacks of parallel β-sheets and their lateral self-assembly, driven by electrostatic interactions and hydrogen bonds. A, F(I)F_water solvate; B, F(I)F pyridine solvate. Color code: C, gray or orange; O, red; N, violet; I, purple; H, white. Hydrogen bonds are shown in light blue dotted lines

phenyl groups of facing dipeptides (Figure 6A). In addition to weak C-H···π interactions, these regions are reinforced by the presence of iodine atoms.

Indeed, the halogens interact each other forming a network of weak type I halogen-halogen contacts and halogen bonds[52] (Figure 6B). The geometrical arrangement of the involved atoms enlightens the peculiar electron density distribution occurring in XB although the contact distances are close to the sum of the van der Waals radii. Specifically, each iodine atom acts as tri-topic ligand, acting as both electrophilic and nucleophilic moieties (distance I···I 3.83 Å, C-I···I angles 158° and 124° for type I contacts; 3.80 Å, 97° and 171° for XB). This arrangement generates hydrophobic channels running along the crystallographic axis *b* and containing the iodine atoms (Figure S7). The segregation of aromatic regions favors the formation of hydrophilic interfaces, where water molecules fill channels parallel to the *b* axis. These solvent molecules are tightly bound to peptide heteroatoms through hydrogen bonds. Solvent voids represent 5.6% of the cell volume for the water solvate of F(I)F (105 $Å^3$), while the region containing iodine atoms is almost 2-fold (11.7%, 221 $Å^3$). The presence of these iodine channels strongly affects the size of the water channels, which instead are much more extended in IFABEW and OREVAK. The different peptide conformation in the pyridine solvate allows the formation of a continuous hydrophobic region, including also channels containing the solvent (Figures 7A, S8). The noniodinated phenyl groups laterally stabilize the peptides strands through C-H···π interactions; on the other side of the F(I)F backbone, the phenyl groups bearing the halogen are involved in weak halogen bonding,[52] as well as in the water solvate (Figure 7B). In this crystal structure, each iodine atom acts as ditopic ligand toward proximate iodine atoms (distance I···I 3.86 Å, angles C-I···I 95° and 160°). Although crystallized under different conditions, both F(I)F structures show extended aromatic regions that are further stabilized by the contribution of halogen bonding, in addition to the typical C-H···π interactions, which are instead the unique stabilizing contacts in IFABEW and OREVAK.

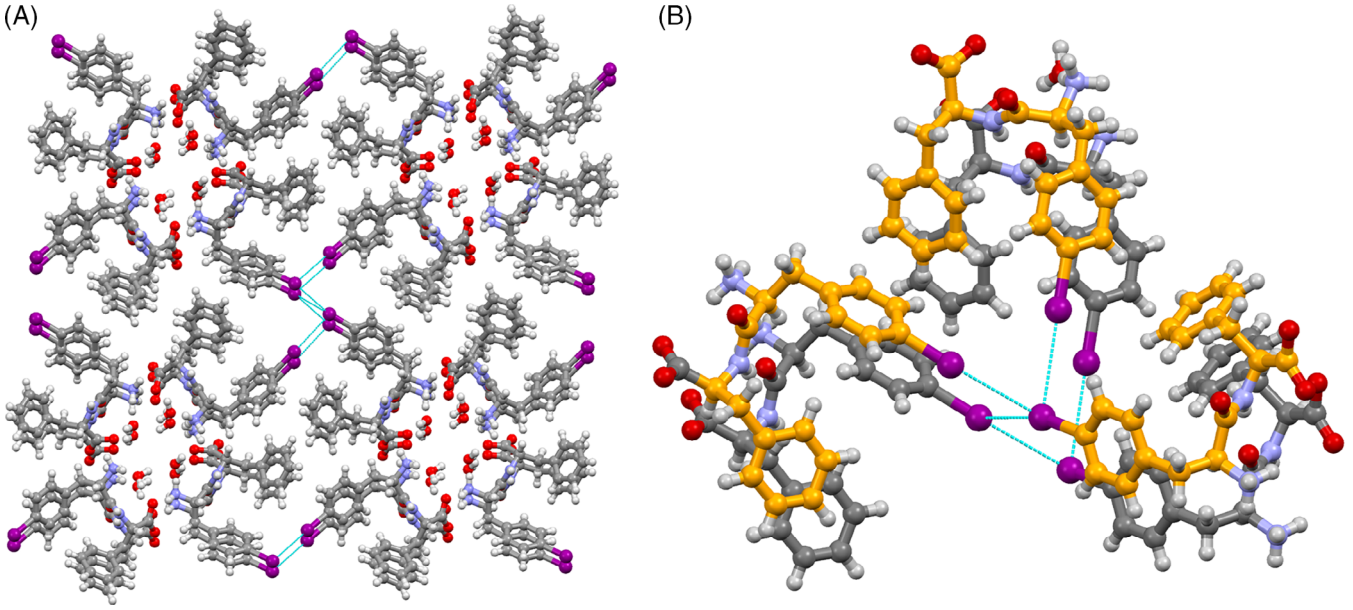


**FIGURE 6** Crystal structure of F(I)F_water solvate. A, Dry interface stabilized by halogen bonds and channels filled by water molecules. B, Focus on the network of type I halogen-halogen contacts and XBs stabilizing the dry interface. Color code: C, gray or orange; O, red; N, violet; I, purple; H, white. Halogen bonds and halogen-halogen contacts are shown in light blue-dotted lines

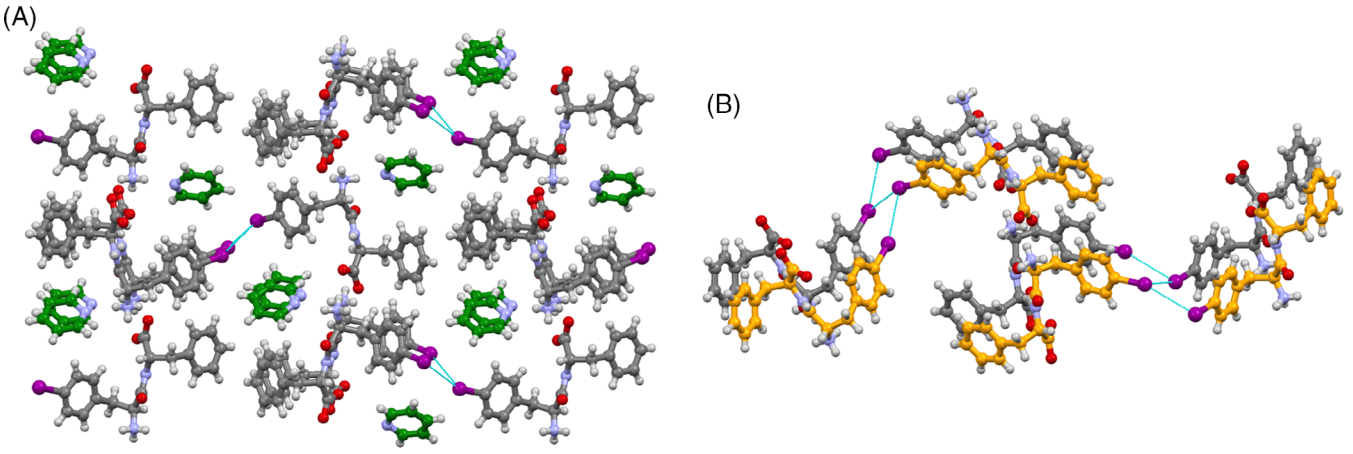


**FIGURE 7** Crystal structure of F(I)F_pyridine solvate. A, Dry interface stabilized by halogen bonds and channels filled by pyridine molecules. B, Focus on the network of XBs stabilizing the dry interface. Color code: C, gray or orange; O, red; N, violet; I, purple; H, white. Halogen bonds are shown in light blue dotted lines

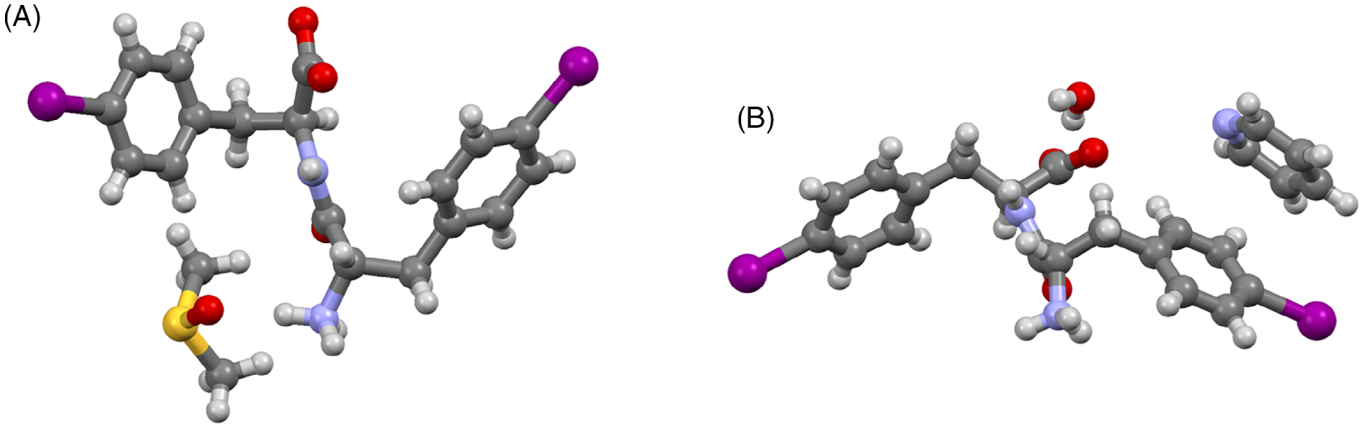


**FIGURE 8** Asymmetric unit content of F(I)F(I) crystal structures. A, DMSO solvate; B, pyridine/water solvate

The bis-iodinated peptide F(I)F(I) was successfully crystallized as solvated species from DMSO and pyridine. The compound crystallizes in the same orthorhombic $P2_12_12_1$ space group in both solvents, with a single peptide molecule in the asymmetric unit (Figure 8).

Similarly to the pyridine solvate of F(I)F, both crystal structures of the bis-iodinated sequence have the phenyl rings located on the opposite sides with respect to the peptide backbone. As shown in the crystal structures of F(I)F, also the bis-iodinated dipeptide stacks in parallel β sheets. Specifically, in the DMSO solvate of F(I)F(I), the parallel β sheets are perfectly in register, stabilized by C-H···O contacts between adjacent strands (C10···O3 3.42 Å, C80···O1 3.29 Å, C13···O3 3.43 Å). Differently, the parallel β sheets formed by the pyridine solvate are out of register and strengthened by hydrogen bonds between the amide nitrogen and the C-terminal carboxylate of stacked molecules (N1···O3 2.88 Å).

The lateral packing in the DMSO solvate is driven by electrostatic interactions, consisting of trifurcated charge-assisted HBs from the N-terminus of the dipeptide with two adjacent carboxylate functionalities and the oxygen of the DMSO molecule (N2···O1 2.77 Å, N2···O2 2.72 Å, N2···O4 2.81 Å, Figure 9A). The crystal packing grows along the crystallographic axis *c*, thanks to the contribution of iodine atoms, stabilizing an extended hydrophobic interface that includes channels filled by the solvent (Figure S9). In detail, the halogen on the N-terminal phenylalanine forms I···S contacts with DMSO (I···S 3.69 Å, C-I···S angle 158°), with sulfur being an electron-rich moiety acting as XB acceptor; on the opposite side of the peptide backbone, the iodine atom on the C-terminal phenylalanine gives rise to I···π interactions with a carbon atom of a facing aromatic ring (I1···C16 distance 3.66 Å). This arrangement induces the formation of infinite domains

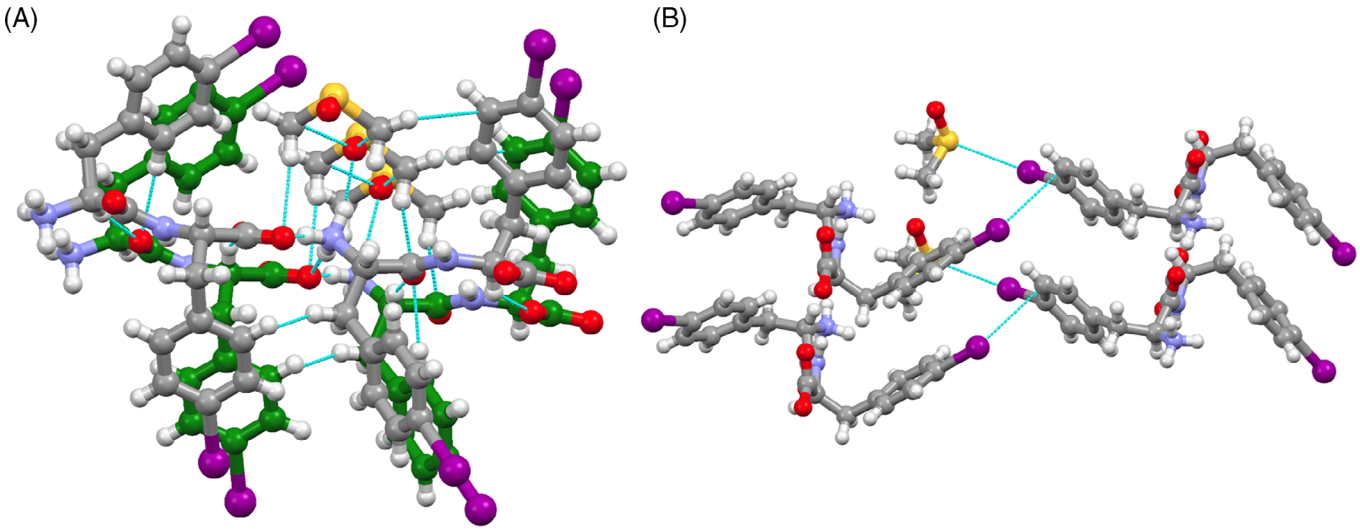


**FIGURE 9** Crystal structure of F(I)F(I)_DMSO solvate. A, In-register parallel β-sheet and their lateral self-assembly, driven by electrostatic interactions and hydrogen bonds. B, Focus on the network of XBs stabilizing the lateral assembly. Color code: C, gray or green; O, red; N, violet; I, purple; H, white. Hydrogen and halogen bonds are shown in light blue dotted lines

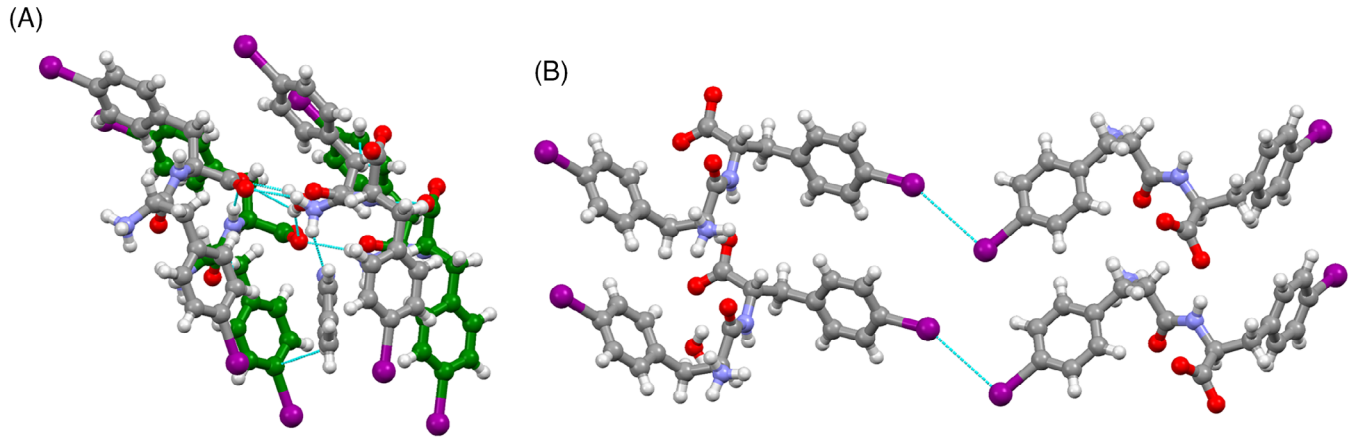


**FIGURE 10** Crystal structure of F(I)F(I)_pyridine solvate. A, Out of register parallel β-sheet and their lateral self-assembly driven by electrostatic interactions and hydrogen bonds. B, Focus on the network of XBs stabilizing the lateral assembly. Color code: C, gray or green; O, red; N, violet; I, purple; H, white. Hydrogen and halogen bonds are shown in light blue dotted lines

containing iodine atoms and growing along the crystallographic axes *b* and *a* (Figure 9B).

The lateral packing of F(I)F(I) crystals obtained from pyridine is driven by a complex network of HBs involving the N-terminus of the dipeptide. Indeed, as in the DMSO solvate, the ammonium group behaves as trifurcated HB donor toward: (a) the aromatic nitrogen of pyridine (N2···N3 distance 2.83 Å); (b) the carboxylate functionality of an adjacent dipeptide monomer (N2···O2 distance 2.91 Å); and (c) the oxygen atom of a water molecule, which is very likely absorbed from the environment (N2···O4 distance 2.69 Å). This water molecule works also as HB donor, interacting with two adjacent carboxylate groups via O-H···O contacts (O4···O2 distance 2.80 Å, O4···O3 distance 2.67 Å), thus stabilizing the β-sheets (Figure 10A).

Even in this crystal structure, iodine atoms contribute to the lateral assembly of the dipeptide chains via halogen bonding interactions (distance I···I 3.94 Å, angles C-I···I 98° and 152°). Also here, the contacts involving iodine atoms are quite weak, the distances being close to the sum of the van der Waals radii. However, like in the DMSO solvate, XBs give an important contribution to reinforce the resulting hydrophobic moiety, which includes pyridine channels and halogen-containing regions (Figures 10B, S10). Also for the bis-iodinated peptide, different crystallization conditions lead to different interaction patterns; however, among the set of noncovalent interaction driving the solid-state packing, halogen bonds—although weak—are always present, conferring additional stability in both crystal structures.

## 4 | CONCLUSION

In conclusion, we have reported a detailed investigation on the role of halogenation in the solid-state assembly of two iodinated derivatives of the diphenylalanine peptide. Our study confirms the great impact of this small, punctual modification on the aggregation of this dipeptide. Varying the number of iodine atoms introduced in the system results into different nanostructures; this confirms the same behavior observed in the halogenated derivatives of the KLVFF peptide, which includes the FF motif in the sequence. In particular, monohalogenation on the N-terminal phenylalanine residue conferred the higher amyloid attitude, as confirmed by TEM images showing bundles of fibrils for F(I)F. The crystal structures here reported are, to the best of our knowledge, the first examples in the CCDC of halogenated diphenylalanines and definitely demonstrate the relevant role of halogen bonding in driving the self-assembly of this small peptide in the solid state. Although the reported crystal structures were obtained under different experimental conditions, XBs were always present, regardless of different structural packings. Specifically, halogenation stabilized the dry interface generated by the affinity among aromatic residues of neighboring peptide molecules. Type I halogen-halogen contacts and XBs give a remarkable contribution to the solid-state packing, working in perfect cooperation and synergy with frequently occurring interactions such as hydrogen bonds and π-π interactions. Although the direct correlation between crystals and noncrystalline nanostructures might be nontrivial, even FT-IR spectroscopy performed on bulk materials suggests the possible role of halogenation in the solid-state assembly. Thus, we consider the reported crystal structures as a reasonable model of the resulting interaction pattern in the presence of highly polarizable halogen atoms. Considering strength and high directionality of halogen bonding, halogenation is not yet fully exploited as a supramolecular tool in the context of peptide-based nanotechnologies; however, we feel that all the potential showed by halogenation will unlock new and valuable opportunities for the scientific community, as shown in the field of catalysis[53] and in the synthesis of hybrid metal-peptide nanostructures.[54]

## ACKNOWLEDGMENTS

The European Research Council is acknowledged for the Starting Grant ERC-2012-StG_20111012 FOLDHALO (Grant Agreement Number 307108) to P.M. and for Proof-of-Concept Grant ERC-2017-PoC MINIRES (Grant Agreement Number 789815) to P.M.

## ORCID

*Andrea Pizzi* https://orcid.org/0000-0002-4180-9151
*Nicola Demitri* https://orcid.org/0000-0003-0288-3233
*Valentina Dichiarante* https://orcid.org/0000-0002-2977-5833
*Giancarlo Terraneo* https://orcid.org/0000-0002-1225-2577
*Pierangelo Metrangolo* https://orcid.org/0000-0002-7945-099X

## REFERENCES

[1] S. Zhang, *Nature Biotechnol.* **2003**, *21*, 1171.
[2] P. Tseng, B. Napier, S. Zhao, A. N. Mitropoulos, M. B. Applegate, B. Marelli, D. L. Kaplan, F. G. Omenetto, *Nature Nanotechnol.* **2017**, *12*, 474.
[3] A. Wang, W. Shi, J. Huang, Y. Yan, *Soft Matter* **2016**, *12*, 337.
[4] C. M. Dobson, *Nature* **2003**, *426*, 884.
[5] Y. Bai, Q. Luo, J. Liu, *Chem. Soc. Rev.* **2016**, *45*, 2756.
[6] P. Makam, E. Gazit, *Chem. Soc. Rev.* **2018**, *47*, 3406.
[7] I. W. Hamley, *Interface Focus* **2017**, *7*, 20170062.
[8] C. J. Bowerman, B. L. Nilsson, *Biopolymers* **2012**, *98*, 169.
[9] E. Gazit, *Chem. Soc. Rev.* **2007**, *36*, 1263.
[10] P. Beker, I. Koren, N. Amdursky, E. Gazit, G. Rosenman, *J Mater Sci.* **2010**, *45*, 6374.
[11] E. De Santis, M. G. Ryadnov, *Chem.Soc.Rev.* **2015**, *44*, 8288.
[12] F. Chiti, C. M. Dobson, *Annu. Rev. Biochem.* **2006**, *75*, 333.
[13] S. Mankar, A. Anoop, S. Sen, S. K. Maji, *Nano Rev.* **2011**, *2*, 6032.
[14] I. Cherny, E. Gazit, *Angew. Chem. Int. Ed.* **2008**, *47*, 4062.
[15] E. Gazit, *Prion* **2007**, *1*, 32.
[16] J.-P. Colletier, A. Laganowsky, M. Landau, M. Zhao, A. B. Soriaga, L. Goldschmidt, D. Flot, D. Cascio, M. R. Sawaya, D. Eisenberg, *Proc. Natl. Acad. Sci. U. S. A.* **2011**, *108*, 16938.
[17] P. W. J. M. Frederix, G. G. Scott, Y. M. Abul-Haija, D. Kalafatovic, C. G. Pappas, N. Javid, N. T. Hunt, R. V. Ulijn, T. Tuttle, *Nat. Chem.* **2015**, *7*, 30.
[18] M. Reches, E. Gazit, *Science* **2003**, *300*, 625.
[19] S. L. Porter, S. M. Coulter, S. Pentlavalli, T. P. Thompson, G. Laverty, *Acta Biomaterialia* **2018**, *77*, 96.

[20] J. Lee, K. Heo, K. Schulz-Schönhagen, J. H. Lee, M. S. Desai, H. Jin, S. Lee, *ACS Nano* **2018**, *12*, 8138.
[21] V. Nguyen, R. Zhu, K. Jenkins, R. Yang, *Nat. Commun.* **2016**, *7*, 13566.
[22] S. Vasilev, P. Zelenovskiy, D. Vasileva, A. Nuraeva, V. Y. Shur, A. L. Kholkin, *J. Phys. Chem. Solids* **2016**, *93*, 68.
[23] Q. Li, Y. Jia, L. Dai, Y. Yang, J. Li, *ACS Nano* **2015**, *9*, 2689.
[24] K. Tao, A. Levin, L. Adler-Abramovich, E. Gazit, *Chem. Soc. Rev.* **2016**, *45*, 3935.
[25] S. Marchesan, A. V. Vargiu, K. E. Styan, *Molecules* **2015**, *20*, 19775.
[26] M. S. Ivanov, V. A. Khomchenko, M. Salimian, T. Nikitinc, S. Kopyl, A. M. Buryakov, E. D. Mishina, F. Salehli, P. A. A. P. Marques, G. Goncalves, R. Fausto, J. A. Paixão, A. L. Kholkin, *Mater. Des.* **2018**, *142*, 149.
[27] A. Mahler, M. Reches, M. Rechter, S. Cohen, E. Gazit, *Adv. Mater.* **2006**, *18*, 1365.
[28] M. Reches, E. Gazit, *Phys. Biol.* **2006**, *3*, S10.
[29] G. Cavallo, P. Metrangolo, R. Milani, T. Pilati, A. Priimägi, G. Resnati, G. Terraneo, *Chem. Rev.* **2016**, *116*, 2478.
[30] A. Pizzi, L. Lascialfari, N. Demitri, A. Bertolani, D. Maiolo, E. Carretti, P. Metrangolo, *CrystEngComm* **2017**, *19*, 1870.
[31] A. Bertolani, L. Pirrie, L. Stefan, N. Houbenov, J. S. Haataja, L. Catalano, G. Terraneo, G. Giancane, L. Valli, R. Milani, O. Ikkala, G. Resnati, P. Metrangolo, *Nat. Commun.* **2015**, *6*, 7574.
[32] A. Bertolani, A. Pizzi, L. Pirrie, L. Gazzera, G. Morra, M. Meli, G. Colombo, A. Genoni, G. Cavallo, G. Terraneo, P. Metrangolo, *Chem. – Eur. J.* **2017**, *23*, 2051.
[33] A. Pizzi, C. Pigliacelli, A. Gori, Nonappa, O. Ikkala, N. Demitri, G. Terraneo, V. Castelletto, I. W. Hamley, F. Baldelli Bombelli, P. Metrangolo, *Nanoscale* **2017**, *9*, 9805.
[34] A. Pizzi, V. Dichiarante, G. Terraneo, P. Metrangolo, *Peptide Science* **2018**, *110*, e23088.
[35] A. Pizzi, N. Demitri, G. Terraneo, P. Metrangolo, *CrystEngComm* **2018**, *20*, 5321.
[36] A. Lausi, M. Polentarutti, S. Onesti, J. R. Plaisier, E. Busetto, G. Bais, L. Barba, A. Cassetta, G. Campi, D. Lamba, A. Pifferi, S. C. Mande, D. D. Sarma, S. M. Sharma, G. Paolucci, *Eur Phys J Plus* **2015**, *130*, 1.
[37] W. Kabsch, *Acta Crystallogr. D* **2010**, *66*, 125.
[38] J. E. McGeehan, P. Carpentier, A. Royant, D. Bourgeois, R. B. G. Ravelli, *J. Synchrotron Rad.* **2007**, *99*, 14.
[39] P. H. Zwart, S. Banumathi, M. Dauter, Z. Dauter, *Acta Crystallogr. D* **2004**, *60*, 1958.
[40] G. M. Sheldrick, *Acta Crystallogr. A* **2015**, *C71*, 3.
[41] G. M. Sheldrick, *Acta Crystallogr. C* **2015**, *A71*, 3.
[42] P. Emsley, B. Lohkamp, W. G. Scott, K. Cowtan, *Acta Crystallogr. D* **2010**, *66*, 486.
[43] G. M. Sheldrick, *Acta Crystallogr. A.* **2008**, *64*, 112.
[44] O. V. Dolomanov, L. J. Bourhis, R. J. Gildea, J. A. K. Howard, H. Puschmann, *J. Appl. Cryst.* **2009**, *42*, 339.
[45] F. Macrae, I. J. Bruno, J. A. Chisholm, P. R. Edgington, P. McCabe, E. Pidcock, L. Rodriguez-Monge, R. Taylor, J. van de Streek, P. A. Wood, *J. Appl. Crystallogr.* **2008**, *41*, 466.
[46] V. Vasylyeva, L. Catalano, C. Nervi, R. Gobetto, P. Metrangolo, G. Resnati, *CrystEngComm* **2016**, *18*, 2247.
[47] A. V. Cunha, E. Salamatova, R. Bloem, S. J. Roeters, S. Woutersen, M. S. Pshenichnikov, T. L. C. Jansen, *J. Phys. Chem. Lett.* **2017**, *8*, 2438.
[48] S. M. Kashid, S. Bagchi, *J. Phys. Chem. Lett.* **2014**, *5*, 3211.
[49] C. H. Görbitz, *Chem. Eur. J.* **2001**, *7*, 5153.
[50] C. H. Görbitz, *Chem. Commun.* **2006**, *22*, 2332.
[51] R. C. Bianchi, E. R. da Silva, L. H. Dall'Antonia, F. F. Ferreira, W. A. Alves, *Langmuir* **2014**, *30*, 11464.
[52] P. Metrangolo, G. Resnati, *IUCrJ* **2014**, *1*, 5.
[53] G. Bergamaschi, L. Lascialfari, A. Pizzi, M. I. Martinez Espinoza, N. Demitri, A. Milani, A. Gori, P. Metrangolo, *Chem. Commun.* **2018**, *54*, 10718.
[54] C. Pigliacelli, K. Buntara Sanjeeva, Nonappa, A. Pizzi, A. Gori, F. Baldelli Bombelli, P. Metrangolo, *ACS Nano* **2019**, *13*, 2158.

## SUPPORTING INFORMATION

Additional supporting information may be found online in the Supporting Information section at the end of this article.

**How to cite this article:** Pizzi A, Catalano L, Demitri N, Dichiarante V, Terraneo G, Metrangolo P. Halogen bonding as a key interaction in the self-assembly of iodinated diphenylalanine peptides. *Peptide Science*. 2020;112:e24127. https://doi.org/10.1002/pep2.24127